

## Direct Correlation Function of a Crystalline Solid

S.-C. Lin<sup>\*</sup> and M. Oettel*Institut für Angewandte Physik, Universität Tübingen, Auf der Morgenstelle 10, 72076 Tübingen, Germany*

J. M. Häring, R. Haussmann, and M. Fuchs

*Fachbereich für Physik, Universität Konstanz, 78457 Konstanz, Germany*

G. Kahl

*Institut für Theoretische Physik, TU Wien, 1040 Vienna, Austria* (Received 26 April 2021; accepted 19 July 2021; published 18 August 2021)

Direct correlation functions (DCFs), linked to the second functional derivative of the free energy with respect to the one-particle density, play a fundamental role in a statistical mechanics description of matter. This holds, in particular, for the ordered phases: DCFs contain information about the local structure including defects and encode the thermodynamic properties of crystalline solids; they open a route to the elastic constants beyond low temperature expansions. Via a demanding numerical approach, we have explicitly calculated for the first time the DCF of a solid: based on the fundamental measure concept, we provide results for the DCF of a hard sphere crystal. We demonstrate that this function differs at coexistence significantly from its liquid counterpart—both in shape as well as in its order of magnitude—because it is dominated by vacancies. We provide evidence that the traditional use of liquid DCFs in functional Taylor expansions of the free energy is conceptually wrong and show that the emergent elastic constants are in good agreement with simulation-based results.

DOI: 10.1103/PhysRevLett.127.085501

*Introduction.*—In classical and quantum theories of many-body systems, two-point correlation functions or propagators play a very important role. In homogeneous systems, they describe the fundamental structural correlations; they can be interpreted as the probability of finding two particles at two different points (in general, these are points in space and time). In functional formulations of many-body theory, these two-point functions are generically related to functional derivatives of a generating functional with respect to two local source terms. In classical systems in equilibrium [1], the generating functional may be taken as the grand potential  $\Omega$  and the source term is the local chemical potential defined by  $\psi(\mathbf{r}) = \beta\mu - \beta V^{\text{ext}}(\mathbf{r})$ , where  $\beta = 1/(kT)$  is the inverse temperature,  $\mu$  is the bulk chemical potential, and  $V^{\text{ext}}(\mathbf{r})$  is an external potential acting on particles at space point  $\mathbf{r}$ . The corresponding second derivative  $-\beta\delta^2\Omega/[\delta\psi(\mathbf{r}_1)\delta\psi(\mathbf{r}_2)] = G(\mathbf{r}_1, \mathbf{r}_2)$  is the total pair correlation function. Upon a Legendre transform to a free energy  $\mathcal{F}[\rho(\mathbf{r})]$  with the one-particle density  $\rho(\mathbf{r})$  as its natural source term variable, another correlation function may be defined by  $\beta\delta^2\mathcal{F}/[\delta\rho(\mathbf{r}_1)\delta\rho(\mathbf{r}_2)] = C(\mathbf{r}_1, \mathbf{r}_2)$ .  $C(\mathbf{r}_1, \mathbf{r}_2) = C^{\text{id}}(\mathbf{r}_1, \mathbf{r}_2) - c(\mathbf{r}_1, \mathbf{r}_2)$  is commonly split into a trivial ideal gas part [ $C^{\text{id}}(\mathbf{r}_1, \mathbf{r}_2) = \delta(\mathbf{r}_1 - \mathbf{r}_2)/\rho(\mathbf{r}_1)$ ] and an excess part, the latter of which is called the direct correlation function (DCF). This function is more fundamental than  $G$ , in the sense that  $G$  may be built by a sequence of the DCFs through the (inhomogeneous) Ornstein-Zernike

relation. Knowing  $c(\mathbf{r}_1, \mathbf{r}_2)$  for the stable phases or aggregate states of classical systems thus entails knowing the structural order of these phases and constitutes a desirable scientific asset. In past decades, the total pair and direct correlations of simple and complex *liquids* have been studied in detail and qualitative and quantitative aspects of them are known [2]. In contrast, this is not the case for the *crystalline* state, whose ordered nature is frequently only characterized by the periodicity in  $\rho(\mathbf{r})$  [which is the first derivative  $-\beta\delta\Omega/\delta\psi(\mathbf{r})$ ]. Here, we aim to close this knowledge gap on the DCF and demonstrate that the shape of a crystal DCF is very different from a liquid DCF and, in particular, is divergent in the limit of an ideal, defect-free crystal. Furthermore, we analyze (generalized) elastic constants, viz. thermodynamic derivatives with respect to density and strain, in terms of the crystal DCF and show that this function encodes the mechanical properties.

*Basic concepts.*—From density functional theory, the appropriate functional expansion of the excess part (over ideal gas) of the free energy around a reference bulk state with density  $\rho_0$  is given by [1]

$$\begin{aligned} \mathcal{F}^{\text{ex}}[\rho] = & F^{\text{ex}}(\rho_0) + \int d\mathbf{r} \mu^{\text{ex}}(\mathbf{r}; \rho_0) \Delta\rho(\mathbf{r}) \\ & - \frac{1}{2\beta} \int d\mathbf{r}_1 \int d\mathbf{r}_2 c(\mathbf{r}_1, \mathbf{r}_2; \rho_0) \Delta\rho(\mathbf{r}_1) \Delta\rho(\mathbf{r}_2) \\ & + \dots \end{aligned} \quad (1)$$

Here,  $F^{\text{ex}}(\rho_0)$  is the excess part of the free energy of the reference state. For a liquid,  $\rho_0$  is constant and  $\mu^{\text{ex}}$  is the constant excess chemical potential, while for a crystal,  $\rho_0$  and  $\mu^{\text{ex}}$  are lattice periodic functions.  $c(\mathbf{r}_1, \mathbf{r}_2; \rho_0)$  is the DCF of the reference state. In many theoretical works, the classical solid is considered as a perturbation of the homogeneous liquid. In Eq. (1) this amounts to approximate  $c(\mathbf{r}_1, \mathbf{r}_2; \rho_0) \approx c^{\text{liq}}(|\mathbf{r}_1 - \mathbf{r}_2|; \rho_0)$  with the translation invariant DCF of the liquid. Minimizations of such a liquidlike free energy functional can qualitatively (e.g., hard sphere systems [3]) and, for some systems, also quantitatively (e.g., soft systems [4–6]) describe crystals with a periodic  $\rho(\mathbf{r})$ ; the underlying assertion is, however, that the crystal DCF is liquidlike.

Earlier fundamental considerations [7] cast doubts on this approach but actual evaluations of the crystal DCF were restricted to a harmonic model.

For a density distribution  $\rho(\mathbf{r})$  with lattice periodicity, the Fourier modes are discrete, nonzero only for reciprocal lattice vectors (RLVs)  $\mathbf{g}$ . The corresponding crystal DCF  $c^{\text{cr}}(\mathbf{r}_1, \mathbf{r}_2)$  is invariant with respect to a global translation by a lattice vector  $\mathbf{L}$ , i.e.,  $c^{\text{cr}}(\mathbf{r}_1 + \mathbf{L}, \mathbf{r}_2 + \mathbf{L}) = c^{\text{cr}}(\mathbf{r}_1, \mathbf{r}_2)$ . We can define center of mass and relative coordinates by  $\mathbf{s}_{12} = \gamma\mathbf{r}_1 + \gamma'\mathbf{r}_2$  and  $\mathbf{r}_{12} = \mathbf{r}_1 - \mathbf{r}_2$  [here,  $\gamma = (1 - \gamma')$  is arbitrary]. Thus the crystal DCF possesses an expansion [7,8]

$$c^{\text{cr}}(\mathbf{r}_1, \mathbf{r}_2) = \sum_{\mathbf{g}} \int \frac{d\mathbf{k}}{(2\pi)^3} e^{i\mathbf{g}\cdot\mathbf{s}_{12}} e^{i\mathbf{k}\cdot\mathbf{r}_{12}} \tilde{c}_{\mathbf{g}}^{\text{cr}}(\mathbf{k}), \quad (2)$$

which defines the RLV modes  $\tilde{c}_{\mathbf{g}}^{\text{cr}}(\mathbf{k})$  of the DCF, where  $\tilde{c}_{\mathbf{g}=\mathbf{0}}^{\text{cr}}(\mathbf{k})$  is the Fourier transform of a translationally invariant  $c(|\mathbf{r}_1 - \mathbf{r}_2|; \rho_0)$ . Equation (1) with  $c(\mathbf{r}_1, \mathbf{r}_2) \approx c^{\text{liq}}(|\mathbf{r}_1 - \mathbf{r}_2|)$  fails fundamentally in considering exclusively this term. Later work [9] pointed out the importance of nonliquidlike parts in the DCF to explain the occurrence of liquid-fcc vs liquid-bcc transitions. The nonliquidlike parts in a restricted expansion have been evaluated using liquid-state methods [10].

There are further arguments showing that the approximation of crystal DCFs by their liquid counterparts should be considered conceptually wrong. The functional definition of  $C$  entails that  $C(\mathbf{r}_1, \mathbf{r}_2) = \delta\psi(\mathbf{r}_1)/\delta\rho(\mathbf{r}_2)$  and describes the change in chemical potential at one point upon change of density at another point. Solids of particles with repulsive cores usually have very few vacancies (their relative concentration  $n_{\text{vac}} \sim 10^{-4}$ ). It can be shown that for a bulk solid of hard spheres  $\psi(\mathbf{r}) = \beta\mu \propto -\ln n_{\text{vac}}$  [11]; i.e.,  $\psi$  diverges for an ideal, defect-free crystal. A local change in density of the crystal should mainly be affected through a change in  $n_{\text{vac}}$  and thus we expect the value of the DCF  $O(c^{\text{cr}}) \sim 1/n_{\text{vac}} \approx 10^4$ , about 2 orders of magnitude larger than the DCF of the hard sphere liquid. Moreover, according to Eq. (1), changes in free energy upon small

density changes in the solid through deformations should be describable with just the crystal DCF at the reference point. This entails a relationship of all the elastic constants to  $c^{\text{cr}}$ . Therefore, the correct nature of the crystalline DCF should also be reflected in measurable quantities.

*Direct correlation function from fundamental-measure theory.*—Below we analyze the crystal DCF of hard spheres with a density functional from fundamental-measure theory (FMT), currently the most accurate density-functional theory available. The so-called dimensional crossover route of derivation of these FMT functionals [12] entails that the free energy of highly localized density profiles is exact. This is crucial for the description of crystals where the density is sharply peaked at lattice sites.

In FMT, the excess free energy is described by a local functional in a set of weighted densities (labeled by  $\alpha$ ),  $n_{\alpha}(\mathbf{r}) = \int d\mathbf{r}_1 \rho(\mathbf{r} - \mathbf{r}_1) w_{\alpha}(\mathbf{r}_1)$  with  $w_{\alpha}(\mathbf{r})$  being a corresponding weight function, defined by geometrical characteristics of the particles [13]

$$\beta\mathcal{F}^{\text{ex}}[\rho] = \int d\mathbf{r} \Phi[n_{\alpha}(\mathbf{r})]. \quad (3)$$

Here we use the White-Bear-II (WBII) tensorial version [14,15] for  $\Phi$  (the full definition is given in the Supplemental Material [16]). Crystal density distributions, the equation of state of both liquid and crystal, and, consequently, the coexistence densities of the liquid and solid are in excellent agreement with simulations [11]. We expect that different variants of FMT functionals that share the correct description of single, localized density peaks could also be used for the present investigation [24,25]. The full minimization in FMT is a two-step process: at a given bulk density, one fixes the average number of particles in the unit cell and minimizes with respect to the density profile under this constraint. In a second step, one minimizes with respect to the average number of particles in the unit cell (i.e., with respect to  $n_{\text{vac}}$ ). Coexistence is determined via the Maxwell construction, and thus one finds the WBII melting point with  $\eta = 0.545$  and  $n_{\text{vac}} = 2.18 \times 10^{-5}$ ; see [11] for details. The crystal DCF follows from the second functional derivative of  $\mathcal{F}^{\text{ex}}$  with respect to  $\rho$

$$c^{\text{cr}}(\mathbf{r}_1, \mathbf{r}_2) = -\sum_{\alpha\beta} \int d\mathbf{r} \frac{\partial^2 \Phi(\mathbf{r})}{\partial n_{\alpha} \partial n_{\beta}} w_{\alpha}(\mathbf{r} - \mathbf{r}_1) w_{\beta}(\mathbf{r} - \mathbf{r}_2), \quad (4)$$

which can most conveniently be analyzed in reciprocal space [16]. We determine  $c^{\text{cr}}$  by two different ways, on the one hand, from the RLV expansion of a fcc lattice and, on the other hand (as a cross-check), via brute force six-dimensional Fourier transformation, both at the WBII melting point.

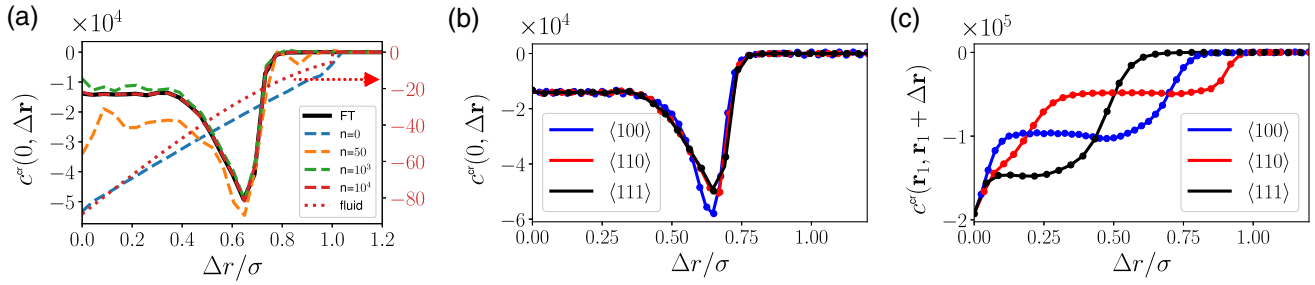


FIG. 1. Direct correlation function  $c^{\text{cr}}(\mathbf{r}_1, \mathbf{r}_2)$  from FMT as function of distance (with  $\sigma$  the sphere diameter) in a hard sphere fcc crystal at the melting density ( $\eta = 0.545$ ,  $n_{\text{vac}} = 2.18 \times 10^{-5}$ ). (a)  $c^{\text{cr}}$  in the RLV expansion up to  $10^4$  shells;  $\Delta\mathbf{r}$  is started from a lattice site. The black solid line is from the brute force FT and the red dotted line is the fluid DCF [26] at  $\eta = 0.545$  with scale on the right side. (b)  $c^{\text{cr}}(0, \Delta\mathbf{r})$  in three directions by the brute force FT (solid line) and RLV expansion up to  $10^4$  shells (dots). (c)  $c^{\text{cr}}(\mathbf{r}_1, \mathbf{r}_1 + \Delta\mathbf{r})$  with distance measured from the interstitial point  $\mathbf{r}_1 = [(a/4), (a/4), (a/4)]$  and  $a$  the side length of the cubic unit cell, lines are as in (b).

Results are shown in Fig. 1. Figure 1(a) shows  $c^{\text{cr}}(0, \Delta\mathbf{r})$ , where the first point (origin) is a lattice point and  $\Delta\mathbf{r}$  points in  $\langle 111 \rangle$  direction of the fcc cubic unit cell. The number  $n$  of RLV shells considered (see the legend) demonstrates the slow convergence of the RLV expansion (we used up to  $n = 10^4$  RLV shells) toward the result obtained from the brute force Fourier transform (FT). The translationally invariant RLV mode  $\tilde{c}_{\mathbf{g}=0}^{\text{cr}}(n=0)$  describes the direct correlations with the center-of-mass variable averaged over the unit cell. It has a similar shape as the fluid DCF but is more than a factor 500 larger [note the separate axis scale for the fluid DCF in Fig. 1(a)]. The shape of the full result is, however, very different from the fluid DCF. Figure 1(b) shows  $c^{\text{cr}}(0, \Delta\mathbf{r})$  using the RLV expansion and the brute force FT in the directions of  $\langle 100 \rangle$ ,  $\langle 110 \rangle$ , and  $\langle 111 \rangle$ . These results demonstrate that the DCF is fairly isotropic around a lattice point. In contrast, the isotropy is lost if an interstitial point is chosen as the first point; see Fig. 1(c), which shows  $c^{\text{cr}}(\mathbf{r}_1, \mathbf{r}_1 + \Delta\mathbf{r})$  in the three directions with  $\mathbf{r}_1 = [(a/4), (a/4), (a/4)]$  ( $a$  is the side length of the cubic unit cell). Overall, the order of magnitude for  $O(c^{\text{cr}}) \sim 10^4$  agrees very well with the estimate  $1/n_{\text{vac}}$  from above, and the 3D spatial dependence is very different from a liquid DCF.

It would be of interest to test the FMT predictions by inversion of the inhomogeneous Ornstein-Zernike (OZ) equation [1] using simulation generated results for the total pair correlation function  $G(\mathbf{r}_1, \mathbf{r}_2)$ . Yet, this approach faces serious numerical pitfalls: simulation results are affected by limited statistics, data for  $G(\mathbf{r}_1, \mathbf{r}_2)$  are available up to distances where this function still shows pronounced oscillations, and the convolution in the OZ equation has to be carried out in full three dimensions.

*Elastic constants.*—The calculation of macroscopic properties of a crystal from first principles requires a correct description of the microscopic structure. Having done the first step, we can explore the ramifications of the discussed DCF properties for the elastic constants (we call this the DCF route to elastic constants). This has been done

so far by using the fluid DCF only [27–30]. The familiar elastic constants are defined through an expansion of the free energy  $F(\eta)$  of a strained crystal to second order in the Lagrangian strain tensor  $\eta_{\alpha\beta} = (u_{\alpha\beta} + u_{\beta\alpha} + u_{\gamma\alpha}u_{\gamma\beta})/2$ , where  $u_{\alpha\beta}$  is the usual gradient of the displacement field ( $u_{\alpha\beta} = \nabla_{\beta}u_{\alpha}$ ) and like indices are summed over [31]

$$\frac{F(\eta)}{V} \approx \frac{F(0)}{V} - p \eta_{\alpha\beta} \delta_{\alpha\beta} + \frac{1}{2} C_{\alpha\beta\gamma\delta} \eta_{\alpha\beta} \eta_{\gamma\delta}. \quad (5)$$

Here,  $V$  is the volume of the unstrained equilibrium reference state with pressure  $p$  and the number of particles is fixed. For a fcc crystal, there are only three independent elastic constants which in Voigt notation are  $C_{11} = C_{\alpha\alpha\alpha\alpha}$ ,  $C_{12} = C_{\alpha\alpha\beta\beta}$ ,  $C_{44} = C_{\alpha\beta\alpha\beta}$  (no summation and  $\alpha \neq \beta$ ). Since a free energy change to second order in strain is equivalent to a change in second order in the density profile [see Eq. (1)], the elastic constants should be expressible with just the density profile and the DCF at the reference state. For the change in density  $\delta\rho(\mathbf{r})$  upon applying a linear displacement field  $\mathbf{u}(\mathbf{r})$  and a change in average density  $\delta\bar{\rho}(\mathbf{r})$ , one may write [32]

$$\delta\rho(\mathbf{r}) \approx -\mathbf{u}(\mathbf{r}) \cdot \nabla\rho(\mathbf{r}) + \rho(\mathbf{r}) \frac{\delta\bar{\rho}(\mathbf{r})}{\bar{\rho}}. \quad (6)$$

While the density profile  $\rho(\mathbf{r})$  varies rapidly on the length scale of the lattice spacing, the coarse-grained displacement and average density field only exhibit smooth variations. This ansatz corresponds to an affine deformation of the crystal density profile. The change in average density  $\bar{\rho}$  is the sum of two effects: the change in vacancy concentration (or occupancy of the unit cell) and the change of the unit cell volume [33,34]. Using this affine approximation, the second-order change in total free energy can be decomposed (see Refs. [8,35])

$$\begin{aligned}\Delta\mathcal{F}^{(2)} &= \frac{1}{2\beta} \int d\mathbf{r}_1 \int d\mathbf{r}_2 \left( \frac{\delta(\mathbf{r}_1 - \mathbf{r}_2)}{\rho(\mathbf{r}_1)} - c^{\text{cr}}(\mathbf{r}_1, \mathbf{r}_2) \right) \\ &\quad \times \delta\rho(\mathbf{r}_1)\delta\rho(\mathbf{r}_2) \\ &= \frac{1}{2} \int d\mathbf{r} \left[ \lambda_{\alpha\beta\gamma\delta} u_{\gamma\alpha} u_{\delta\beta} - 2\mu_{\alpha\beta} \frac{\delta\bar{\rho}}{\bar{\rho}} u_{\beta\alpha} + \nu \left( \frac{\delta\bar{\rho}}{\bar{\rho}} \right)^2 \right].\end{aligned}\quad (7)$$

This defines the generalized elastic constants as thermodynamic derivatives

$$\begin{aligned}\lambda_{\alpha\beta\gamma\delta} &= \frac{1}{2} \hat{I} [\nabla_\alpha \rho(\mathbf{r}_1) \nabla_\beta \rho(\mathbf{r}_2) c^{\text{cr}}(\mathbf{r}_1, \mathbf{r}_2) r_{12,\gamma} r_{12,\delta}], \\ \mu_{\alpha\beta} &= \hat{I} [\rho(\mathbf{r}_1) \nabla_\alpha \rho(\mathbf{r}_2) c^{\text{cr}}(\mathbf{r}_1, \mathbf{r}_2) r_{12,\beta}], \\ \nu &= \hat{I} \left[ \rho(\mathbf{r}_1) \left( \frac{\delta(\mathbf{r}_{12})}{\rho(\mathbf{r}_2)} - c^{\text{cr}}(\mathbf{r}_1, \mathbf{r}_2) \right) \rho(\mathbf{r}_2) \right],\end{aligned}\quad (8)$$

with the integral operator  $\hat{I} = (1/V\beta) \iint d\mathbf{r}_1 d\mathbf{r}_2$  and  $\mathbf{r}_{12} = \mathbf{r}_1 - \mathbf{r}_2$  with Cartesian components  $r_{12,\alpha}$ . According to Eq. (6), these generalized elastic constants have the following meaning: the  $\lambda$ 's are the constants sensitive to a second-order density profile variation due to a combination of “strain-strain,” the  $\mu$ 's accordingly are sensitive to “strain-average density change,” and  $\nu$  is sensitive to the combination “average density change–average density change.” It follows that for a defect-free crystal ( $n_{\text{vac}} \rightarrow 0$ ) some of the generalized coefficients must become very large, since in such a case an independent variation of strain or average density would always be accompanied with a creation of interstitials whose free energy cost is large [36].

The standard elastic constants in Voigt notation are a suitable combination of the generalized constants reflecting the process of stressing the crystal without the constraint of fixed density (see the Supplemental Material [16]),

$$\begin{aligned}C_{11} &= \lambda_{xxxx} + 2\mu_{xx} + \nu + p, \\ C_{12} &= 2\lambda_{xyxy} - \lambda_{xxyy} + 2\mu_{xx} + \nu - p, \\ C_{44} &= \lambda_{xxyy} + p,\end{aligned}\quad (9)$$

with  $p$  as the pressure. Note that Eq. (9) also requires one to pass from linear to Lagrange strain [31] and that the volume of the integration in Eq. (7) differs from the volume of the reference state used in Eq. (5).

The computation of the (generalized) elastic constants using the RLV modes of the FMT functional is described in the Supplemental Material [16]. Their dependence on the vacancy density can be studied through employing a crystal density profile at fixed  $n_{\text{vac}}$  and subsequently computing the DCF and the integrals of Eq. (8). The constrained crystal density profile is obtained by the first step of the two-step minimization procedure with a fixed number of particles in the unit cell [11]. In Fig. 2(a), the generalized elastic constants are shown for different  $n_{\text{vac}}$  at coexistence ( $\eta = 0.545$ ). Except for  $\lambda_{xxyy}$ , these are  $\propto 1/n_{\text{vac}}$  in agreement with our reasoning above.  $\lambda_{xxyy}$  is comparably small and insensitive to changes in  $n_{\text{vac}}$ . As it describes the response to shear strains that do not generate defects, i.e., do not create interstitials, this result also agrees with our expectation. Note that an evaluation of the generalized elastic constants by using a liquidlike DCF in Eq. (8) gives results almost independent on vacancy concentration; see the dotted lines in Fig. 2(a). Clearly, a fluid DCF qualitatively fails to describe the thermodynamic derivatives approaching the ideal crystal limit.

Interestingly, the Voigt elastic constants from the DCF route [Eq. (9), see Fig. 2(b)] remain almost unchanged for  $n_{\text{vac}}$  up to  $10^{-2}$ , as a result of a delicate cancellation between the generalized elastic constants, which vary from  $10^4$  to  $10^2$ . The insensitivity of the elastic constants to local defects explains why previous calculations of the Voigt constants using a liquidlike DCF gave qualitatively

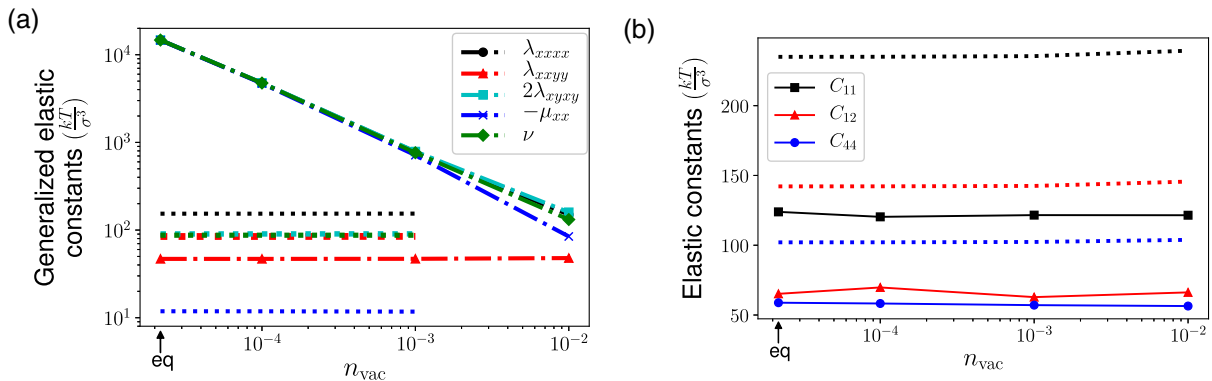


FIG. 2. DCF route to elastic constants: (a) generalized elastic constants and (b) Voigt elastic constants at coexistence ( $\eta = 0.545$ ) as a function of vacancy concentration. Symbols connected with full lines are results from Eqs. (8) and (9), and dotted lines use Eqs. (8) and (9) with  $c^{\text{cr}}(\mathbf{r}_1, \mathbf{r}_2) \rightarrow c^{\text{liq}}(|\mathbf{r}_1 - \mathbf{r}_2|; \eta_0)$ , the fluid DCF [26] at  $\eta_0 = 0.545$ ; “eq” with the arrow indicates the equilibrium  $n_{\text{vac}}$ .

TABLE I. Elastic constants from the DCF route, explicit deformations (FMT), and simulation [36] at the melting point. All elastic constants are defined using Eq. (5). The melting point packing fractions is at  $\eta = 0.543$  in simulations [36] and at  $\eta = 0.545$  in FMT.

	DCF	Deformation (FMT)	Simulation
$\frac{1}{3}C_{11} + \frac{2}{3}C_{12}$	82.63	$38.4 \pm 0.4$	$37.15 \pm 0.07$
$C_{11} - C_{12}$	63.12	$61.9 \pm 0.4$	$52.19 \pm 0.44$
$C_{44}$	58.81	$49.5 \pm 0.5$	$44.67 \pm 0.11$

reasonable behavior. Yet, quantitatively, the liquid DCF gives values off by a factor of 2; see the dotted lines in Fig. 2(b).

Additionally, we compare the Voigt elastic constants from the DCF route with the ones obtained by an explicit free energy determination of suitably deformed unit cells and using Eq. (5). For the choice of deformations, we follow the procedure proposed in Ref. [37] (see the Supplemental Material [16] for details) and perform a free minimization of the free energy without resorting to density profile parametrizations. In view of the high accuracy of the free energy for equilibrium crystals [11], this should constitute a reliable benchmark. In Table I, results from the DCF route and from explicit deformations in FMT are shown and compared with simulations [36] at the melting point. Note that the particular linear combinations of elastic constants in Table I distinguish between a compression mode (volume change) of the fcc crystal, viz. the bulk modulus  $\frac{1}{3}C_{11} + \frac{2}{3}C_{12}$ , and two modes with no volume change through  $C_{11} - C_{12}$  (expansion in one Cartesian direction and compression in another) and  $C_{44}$  (shear).

For all constants, values at least 2 orders of magnitude smaller than the defect-dominated strain derivatives are found, and results obtained from the FMT functionals by the two different routes are rather consistent with the simulation data. Differences are largest for the bulk modulus, which apparently changes most during the non-affine relaxation of the free energy; see the Supplemental Material [16] for an explicit calculation. The differences between the two routes point to necessary corrections to the affine approximation of the density profile change in Eq. (6), which is currently under investigation.

*Outlook.*—In this Letter, we have investigated the direct correlation function of the hard sphere solid using state-of-the-art density functionals of FMT type. The crystal DCF is fundamentally different from the one of the hard sphere liquid as density changes require local defects, viz. vacancies, in solids that are close to ideal. The order of magnitude of the DCF is thus proportional to the inverse vacancy concentration. Generalized elastic constants may be defined in terms of the DCF and the crystal density profile and show the proportionality to the inverse vacancy concentration. Liquidlike DCFs do not entail this property. Standard elastic constants are determined by the

deformation of the lattice, while defects can adjust to the strain. Thus these constants take finite values, also in the limit of an ideal crystal. The sensitivity of the generalized elastic constants to defect concentrations suggests the need for a closer look at defect-rich systems in the future such as polydisperse hard spheres (where interstitials will dominate over vacancies [38]), systems of colloidal cubes [39], or interpolating systems to defect-dominated cluster crystals [4]. We anticipate that the generalized constants play a role for solids with impurities and are relevant to mechanochemical coupling in such systems [40].

This work is supported by Deutsche Forschungsgemeinschaft through a D-A-CH Grants No. FU 309/11-1 and No. OE 285/5-1, and the Austrian Funding Agency (FWF) under Grant No. I3846-N36.

\*shang-chun-lin@uni-tuebingen.de

- [1] R. Evans, *Adv. Phys.* **28**, 143 (1979).
- [2] J.-P. Hansen and I. R. McDonald, *Theory of Simple Liquids: With Applications to Soft Matter* (Academic Press, New York, 2013).
- [3] T. V. Ramakrishnan and M. Yussouff, *Phys. Rev. B* **19**, 2775 (1979).
- [4] C. N. Likos, B. M. Mladek, D. Gottwald, and G. Kahl, *J. Chem. Phys.* **126**, 224502 (2007).
- [5] D. Pini, A. Parola, and L. Reatto, *J. Chem. Phys.* **143**, 034902 (2015).
- [6] B. M. Mladek, D. Gottwald, G. Kahl, M. Neumann, and C. N. Likos, *Phys. Rev. Lett.* **96**, 045701 (2006); **97**, 019901 (E) (2006).
- [7] J. S. McCarley and N. W. Ashcroft, *Phys. Rev. E* **55**, 4990 (1997).
- [8] C. Walz and M. Fuchs, *Phys. Rev. B* **81**, 134110 (2010).
- [9] A. S. Bharadwaj, S. L. Singh, and Y. Singh, *Phys. Rev. E* **88**, 022112 (2013).
- [10] A. Jaiswal, A. S. Bharadwaj, and Y. Singh, *J. Chem. Phys.* **140**, 211103 (2014).
- [11] M. Oettel, S. Görig, A. Härtel, H. Löwen, M. Radu, and T. Schilling, *Phys. Rev. E* **82**, 051404 (2010).
- [12] Y. Rosenfeld, M. Schmidt, H. Löwen, and P. Tarazona, *J. Condens. Matter Phys.* **8**, L577 (1996).
- [13] Y. Rosenfeld, *Phys. Rev. Lett.* **63**, 980 (1989).
- [14] P. Tarazona, *Phys. Rev. Lett.* **84**, 694 (2000).
- [15] R. Roth, *J. Phys. Condens. Matter* **22**, 063102 (2010).
- [16] See Supplemental Material at <http://link.aps.org/supplemental/10.1103/PhysRevLett.127.085501> for the full definition and a discussion of the WBII tensorial functional, details of the numerical implementation of DCF and generalized elastic constants, and discussion of the discrepancy in elastic constants between DCF and explicit deformation in density functional theory, which includes Refs. [17–23].
- [17] W. A. Curtin and N. W. Ashcroft, *Phys. Rev. A* **32**, 2909 (1985).
- [18] R. Ohnesorge, H. Löwen, and H. Wagner, *Phys. Rev. A* **43**, 2870 (1991).

- [19] T. Bernet, E. Müller, and G. Jackson, *J. Chem. Phys.* **152**, 224701 (2020).
- [20] M. Mortazavifar, Ph.D. thesis, Eberhard Karls Universität Tübingen, 2016, <https://publikationen.uni-tuebingen.de/xmlui/handle/10900/74611>.
- [21] M. Frigo and S. G. Johnson, *Proc. IEEE* **93**, 216 (2005).
- [22] J. Nickolls, I. Buck, M. Garland, and K. Skadron, *Queueing Syst. Theory Appl.* **6**, 40 (2008).
- [23] D. Stopper and R. Roth, *J. Chem. Phys.* **147**, 064508 (2017).
- [24] H. Hansen-Goos, M. Mortazavifar, M. Oettel, and R. Roth, *Phys. Rev. E* **91**, 052121 (2015).
- [25] J. F. Lutsko, *Phys. Rev. E* **102**, 062137 (2020).
- [26] M. Oettel, S. Dorosz, M. Berghoff, B. Nestler, and T. Schilling, *Phys. Rev. E* **86**, 021404 (2012).
- [27] M. D. Lipkin, S. A. Rice, and U. Mohanty, *J. Chem. Phys.* **82**, 472 (1985).
- [28] M. V. Jarić and U. Mohanty, *Phys. Rev. B* **37**, 4441 (1988).
- [29] M. C. Mahato, H. R. Krishnamurthy, and T. V. Ramakrishnan, *Phys. Rev. B* **44**, 9944 (1991).
- [30] M. P. Tosi and V. Tozzini, *Philos. Mag. B* **69**, 833 (1994).
- [31] D. C. Wallace, *Solid State Phys.* **25**, 301 (1970).
- [32] G. Szamel and M. H. Ernst, *Phys. Rev. B* **48**, 112 (1993).
- [33] P. C. Martin, O. Parodi, and P. S. Pershan, *Phys. Rev. A* **6**, 2401 (1972).
- [34] P. Fleming and C. Cohen, *Phys. Rev. B* **13**, 500 (1976).
- [35] J. M. Häring, C. Walz, G. Szamel, and M. Fuchs, *Phys. Rev. B* **92**, 184103 (2015).
- [36] S. Pronk and D. Frenkel, *Phys. Rev. Lett.* **90**, 255501 (2003).
- [37] B. B. Laird, *J. Chem. Phys.* **97**, 2699 (1992).
- [38] S. Pronk and D. Frenkel, *J. Chem. Phys.* **120**, 6764 (2004).
- [39] F. Smalenburg, L. Filion, M. Marechal, and M. Dijkstra, *Proc. Natl. Acad. Sci. U.S.A.* **109**, 17886 (2012).
- [40] S. Shi, J. Markmann, and J. Weissmüller, *Proc. Natl. Acad. Sci. U.S.A.* **115**, 10914 (2018).